IMECE2003-41680

EFFECTS OF NONCONDENSABLE GAS AND SUBCOOLING ON THE SPRAY COOLING OF AN ISOTHERMAL SURFACE

Bohumil Horacek, Jungho Kim, and Kenneth T. Kiger
Department of Mechanical Engineering
University of Maryland
College Park, MD 20742

ABSTRACT

Spatially resolved heat transfer measurements have been made on a nominally isothermal surface that is spray cooled. The effects of dissolved gas and subcooling were studied. The local measurements were obtained using a microheater array with ninety-six heaters each about 700 microns in size. The heater array consisted of thin-film platinum resistors deposited on a quartz substrate. Electronic feedback circuits were used to keep each of the heaters at a constant temperature and the voltage required to do this was measured. The array was cooled with FC-72 using a spray nozzle from ISR. The heat transfer data was correlated with high-speed images of the flow structure obtained from below. In this paper, heat transfer mechanisms in spray cooling will be discussed, with a particular emphasis on the effects of a non-condensable gas on critical heat flux in comparison to the comparable effects of thermally subcooling the liquid prior to atomization.

NOMENCLATURE

CHF	Critical heat flux
d_{32}	Sauter mean diameter
d_0	nozzle diameter
ΔP	pressure difference across nozzle (N/m^2)
ΔT_{sub}	subcooling [K]
Re	Reynolds number
We	Weber number
σ	surface tension (N/m)
ρ	density (kg/m^3)
μ	dynamic viscosity (Pa-s)

INTRODUCTION

Spray cooling can be used to transfer large amounts of energy at low temperatures through the latent heat of evaporation. Heat transfer rates much higher than can be attained using pool boiling are possible with sprays since the vapor removal from the surface is much easier. A considerable amount of work has been performed on the effects of subcooling on spray heat transfer (e.g., Holman and Kendall-1993, Tilton et al.–1992, Ortiz and Gonzalez–1999, Kendall and Holman, 1996, Chen, et al.–2002, Estes and Mudawar–1995a). All of the results indicate that increasing subcooling leads to an increase in the heat transfer. Very little is known, however, regarding the effects of dissolved gases on spray performance.

Cui, *et al*. (2000) studied the effect of dissolved gases and solid precipitates on droplet heat transfer. Carbon dioxide gas or a salt was dissolved in water and videos of the evaporation process were obtained as the droplets struck a heated surface. For temperatures below and above the boiling point, the dissolved gas (0.74 mm^3/mm^3) was observed to increase the heat transfer slightly due to an increase in the splat circumference. When 1% by weight of $NaHCO_3$ was added to the liquid, it decayed when heated into Na_2CO_3 and CO_2. Foaming within the droplet was observed to occur along with a large increase in heat transfer. Precipitation of Na_2CO_3 salt within the drop served as nucleation sites for boiling, and the CO_2 produced caused the droplet to swell, increasing the contact area.

Milke *et al*. (1997) studied the effects of dissolved gas on spray evaporation using water. A Macor substrate was heated using three radiant panels. They found that cooling with gassy liquid resulted in a lower steady-state average temperatures, but they attributed this to the decrease of radiant energy input to the surface when gassy liquid was used.

Lee, *et al*. (2002) studied heat transfer under drops impacting a constant temperature surface in which bubbles formed due to dissolved gas coming out of solution. In some cases, a large primary bubble formed within the drop and burst

at various times during the evaporation process. Formation of larger bubbles within the drop was found to increase the wall heat transfer and decrease the drop lifetime. The wall heat transfer due to an evaporating drop was found to be primarily dependent on the liquid-vapor contact area, indicating that the vapor removal process was the limiting thermal resistance.

Tilton, *et al*. (1992), in their study of spray cooling concluded that gas degraded the condenser performance to the point where excess fluid removal was inhibited. They also stated that for fixed volume systems, the presence of gas would cause the boiling temperature to increase, increasing the surface temperature. However, a recent study by Lin and Ponnappan (2002) indicated that dissolved air degrades the performance at lower wall temperatures, but the maximum heat transfer is increased compared to sprays without dissolved gas.

The objective of this work is to investigate the effects of dissolved gas on spray cooling heat transfer. Spray cooling curves were obtained on a microfabricated surface that provides a nominally constant temperature boundary condition for the spray. Visualization of the flow on the surface was also performed, and spray cooling heat transfer mechanisms are discussed.

EXPERIMENTAL APPARATUS

The effects of dissolved gas and subcooling were studied using a full cone ISR spray nozzle to cool a microheater array with total area of 0.49 cm^2 (7.0 mm x 7.0 mm). The heater array consisted of 96 heaters each nominally 700 microns in size, configured in a similar arrangement as the 2.6 mm arrays used for previous droplet cooling measurements (Lee, *et al*., 2002). Figure 1 provides an image of the heater array, along with a schematic showing the heater enumeration and the location of inoperable heater elements that occurred during the fabrication process. Each heater element consisted of a thin (200 nm thick, 7 μm wide) serpentine platinum resistance heater than was sputtered on to a tungsten adhesion layer bonded to the 500 μm thick quartz substrate. The effective temperature coefficient of resistance of the metallic layer was approximately 0.002 $°C^{-1}$, with the length, width and thickness of the serpentine elements designed to provide a nominal resistance of approximately 180 Ω. Thicker gold leads were deposited up to the edge of the array to ensure minimal lead resistance (< 1 Ω), and the entire array was covered with a 1 μm SiO_2 passivation layer to provide a surface with uniform surface energy.

Individual heater elements were maintained at a constant specified temperature through the use of 96 separate Wheatstone bridge feedback circuits, as illustrated schematically in Figure 2. The temperature of the element was selected through the use of a 20 kW digital potentiometer that was discretized in 512 discrete steps. When combined with the other resistor elements in the circuit, this provided for an effective temperature regulation range from 30 °C to 110 °C, with a resolution of approximately 0.2 °C. In the current configuration, each heater is capable of dissipating 1.3 W, giving a maximum surface heat flux of up to 250 W/cm^2. The settings for the digital potentiometer were calibrated through the use of a constant-temperature, insulated, calibration oven. A feedback controller was used to maintain a constant interior oven temperature, while the threshold setting of the digital potentiometer that just started regulation of the circuit was determined. The calibration was performed on all heater elements simultaneously, and conducted in 5°C increments over the span of operation. During the experiments, two 64-channel 12-bit analog-to-digital conversion boards were used to sample data from an individual heater at rates of up to 3400 kHz (220 kHz bandwidth on each board).

The use of a transparent quartz substrate combined with the 50% coverage area of the serpentine heater element allowed for the visualization of the impacting spray from beneath the semi-transparent heater array (see Figure 3). A high-speed digital camera (Vision Research Phantom v4.0) capable of acquiring 512x512 pixel images at speeds of up to 1000 fps was used to record the visualizations. The camera was configured to

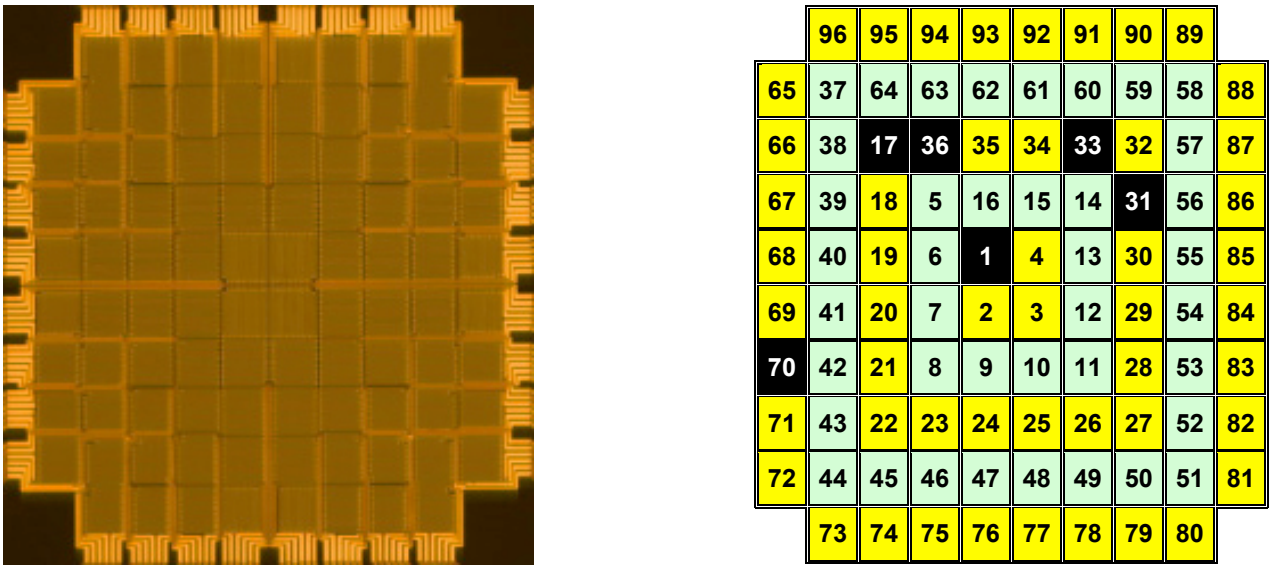

Figure 1: Photograph of heater array (left) and schematic of heater numbering (right). Inoperable heaters are indicated in black.

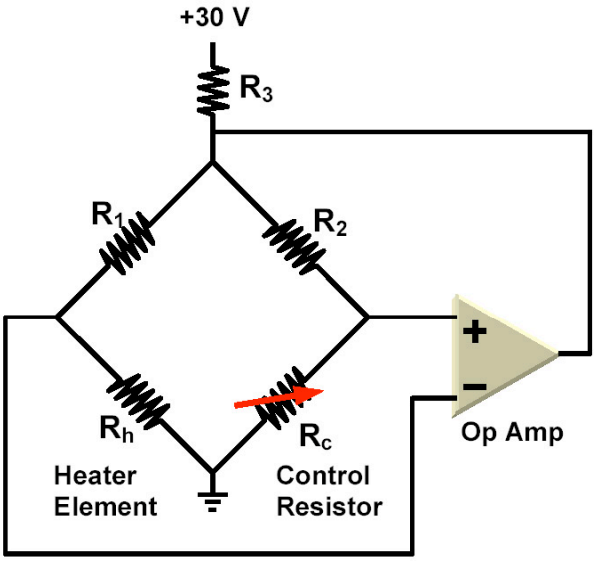

Figure 2: Schematic of feedback control circuit for individual heater element.

run with a reduced sensor size of 128x512 pixels, operating at 3200 fps, and was synchronized to the data acquisition system of the heater array. A tele-microscope lens (Infinity KC with IF3 objective) provided variable magnification imaging (0.9x – 1.3x) with a working distance of 15 to 19 cm. The lens and camera were adjusted to provide an image of 16 heaters in a 2x8 formation on the array surface.

The tests were performed within a closed flow loop consisting of a spray chamber, condenser, and pump (see schematic on Figure 3) with FC-72 as the test fluid. Some properties of FC-72 are summarized in Table 1. The dimensions of the test section are 25 mm wide, 16 mm high, and approximately 180 mm long. Temperature and pressure (Omega PX 212 0-30 psia) measurements were made at the inlet to the spray nozzle and within the liquid reservoir. The pressure was observed to be uniform throughout the flow loop under all conditions tested. Liquid flow to the spray nozzle was measured using a rotameter. The heater array was inclined at a slight angle with respect to the horizontal to help excess fluid that did not vaporize drain through the condenser into the reservoir. The nozzle distance from the heater surface was fixed at 17 mm for all tests. The nozzle diameter was measured from photographs to be d_0=0.2 mm. The pump was a magnetically coupled gear pump with a head capable of pumping up to 50 ml/min. The amount of dissolved gas within the liquid was varied by controlling the pressure within the test section using a vacuum pump. A chiller consisting of a copper coil immersed in an ice bath or LN_2 bath was used in some cases to cool the liquid entering the spray nozzle.

UNCERTAINTY ANALYSIS

The instantaneous power required to keep each heater at a constant temperature was measured and used to determine the heat flux from each heater element. Because all the heaters in the array are at essentially the same temperature, heat conduction between adjacent heaters is negligible. The total

Temperature (°C)	Vapor Pressure (atm)	Density (kg/m^3)	Latent Heat (kJ/kg)	Specific Heat (J/kg-K)
20	0.2323	1692	94.4	1050
30	0.3606	1669	91.8	1050
40	0.5404	1650	89.2	1050
50	0.7850	1631	86.4	1050
56.6	1.000	1620	84.5	1050
60	1.1091	1614	83.5	1050
70	1.5288	1593	80.6	1050

Table 1: Common properties of FC-72.

heat flux measured for each heater (q''_{raw}), however, must be corrected to account for substrate conduction. q''_{raw} can be lost through the bottom by conduction through the substrate (q''_{sc}),or to the spray (q''_{spray}). q''_{sc} for each heater in the array at a set temperature can be determined by setting the heater to the specified temperature and measuring the power required to keep it at that temperature with no spray on the surface. The natural convection from the heater is smaller than 0.1 W/cm^2, much smaller than the measured spray cooling heat fluxes. In all of the cases studied, q''_{sc} was much smaller than q''_{spray} for all heaters except the edge heaters (heaters 65-96 in Figure 1) since the substrate was relatively thin (450 μm) compared to the heater size (700 μm). The edge heaters act as "guard" heaters for the internal heaters (heaters 1-64 on Figure 1), and prevent heat loss through the substrate for the internal heaters. The heat dissipation rate for the edge heaters changes depending on convection mechanism since the heat transfer from the unheated portion of the substrate also changes. In the data discussed below, the heat transfer from the edge heaters has been excluded from the calculations.

The uncertainty in the heat flux due to measurement errors results from uncertainties in q''_{raw} and q''_{sc}. Uncertainties in q''_{raw} are relatively small since they were computed directly from the measured voltage across the heaters and since the heater resistances do not change much. The maximum uncertainty in the voltage across the heater is 0.04 V. The uncertainty in heater resistance is about 1 Ω. Since the heater resistance is nominally 180 Ω, the % uncertainty in heater resistance is about 0.56 %. The resulting uncertainty in heat transfer due to measurement inaccuracies in the feedback circuit and data acquisition system can be conservatively calculated to be less than 3 %.

Larger uncertainties in the spray cooling curve can result from uncertainties in liquid flow rate, wall temperature, and dissolved gas concentration. The liquid flow rate was steady to within 0.5 ml/min (1.4–4.5% over the range of flow rates tested). The uncertainty in wall temperature is assumed to be two positions on the digital potentiometer, or 0.4 °C. The amount of gas in the flow loop can be determined by measuring the pressure and temperature in the flow loop. The *distribution* of the gas, however, can vary within the flow loop if the temperatures vary (as it does since the heater is hotter than the surroundings), making it difficult to quantify the local gas concentration. The accuracy of the pressure transducer used was 1.5 %. Repeated measurements of the spray cooling

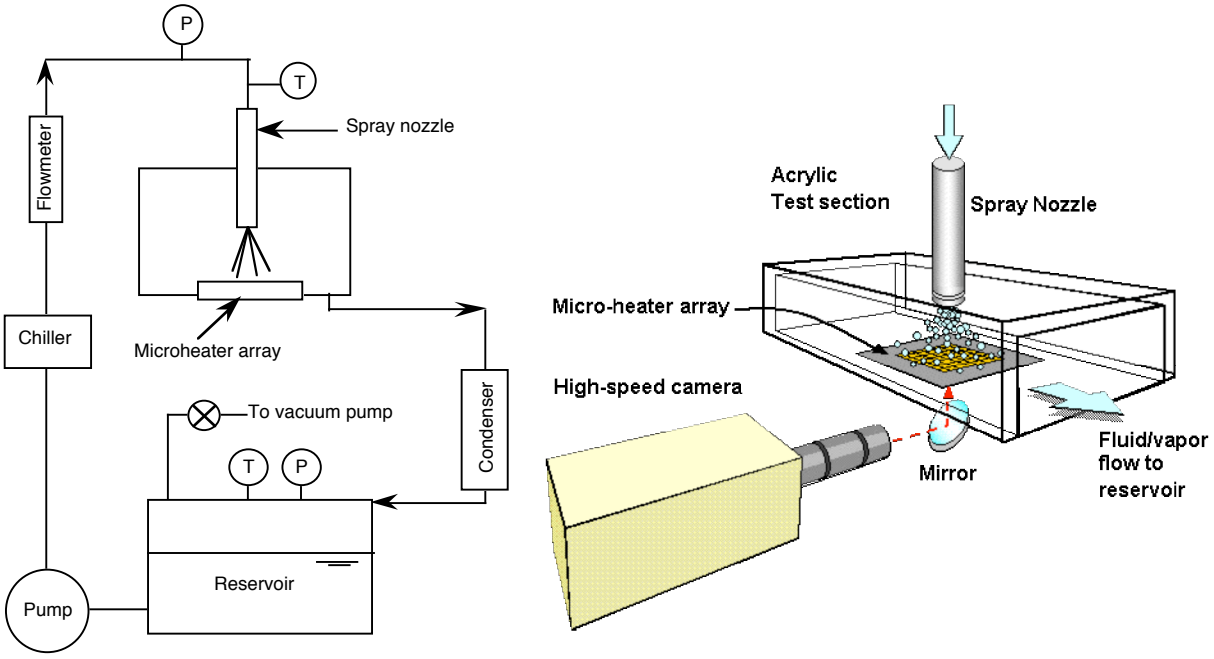

Figure 3: Schematic of test loop facility (left) and detail schematic of test section, spray nozzle, heater and high-speed camera (right).

curves under the same nominal conditions resulted in errors of about 4%. The total uncertainty in the spray cooling curves obtained by combining the uncertainty in repeatability with the measurement inaccuracies is estimated to be 5%.

EFFECT OF GAS

The presence of any non-condensable gas will increase the pressure in the test section above the saturation pressure of the liquid corresponding to the reservoir temperature. Henry's law can be used to determine the amount of dissolved gas in the liquid. The dissolved gas concentration C_g (moles gas/mole liquid) in the liquid phase is given by

$$C_g=H(T)P_g$$

where P_g is the partial pressure of the gas above the liquid and H(T) is Henry's constant. For air in FC-72, this has been measured to be $5.4x10^{-5}$ mole/mole-kPa for 31°C $< T <$ 60°C. P_g can be determined from a measurement of the pressure (P_{tot}) and temperature (T_{sat}) of the gas above the liquid after it has come to equilibrium in a sealed container from the following equation:

$$P_g=P_{tot}-P_{sat}(T_{sat})$$

where P_{sat} is the saturation pressure of the liquid at the measured temperature T_{sat}.

Subcooling of the liquid entering the spray nozzle can be accomplished in two ways. Consider first the case where all gas has been removed from the test section. The pressure in the flow loop then corresponds to the vapor pressure at the temperature of the liquid in the reservoir, and the liquid in the reservoir is at saturated conditions. Liquid can be pumped from the reservoir through a chiller to decrease its temperature before being sprayed on the heater. The liquid sprayed onto the heater is now in a state we will refer to as "thermally subcooled", which will henceforth be referenced as "TS" and is defined as the temperature difference between the reservoir temperature and the initial liquid spray temperature. Consider next the case where air is allowed into the flow loop. The saturation temperature of the liquid in the reservoir has now increased since the pressure above the liquid is higher than the vapor pressure. Even if the liquid from the reservoir is not cooled before entering the spray nozzle, the liquid being sprayed onto the heater will be effectively subcooled since its temperature is below the saturation temperature. The liquid sprayed onto the heater is in a state we will refer to as "gas subcooled", which is similar to the terminology used by Rainey *et al*. (2003) in their studies of gas effects on pool boiling. Henceforth this state will be referenced as "GS", which is defined as the temperature difference between the saturation temperature and the reservoir temperature. The total subcooling (S_{tot}) is defined as S_{tot}=TS+GS.

It is seen from the above discussion that one of the primary effects of the non-condensable gas is to change the saturation temperature of the liquid, and therefore the amount by which the liquid being sprayed on the surface is subcooled for a constant spray temperature. For example, consider the case where liquid FC-72 is at 22 °C in the reservoir. If the flow loop is at 1 atm due to the presence of gas (T_{sat}=56.6 °C) and liquid from the reservoir is sprayed onto the heater, the liquid will be gas subcooled by GS=34.6 °C (=56.6-22). If the gas is now completely removed from the flow loop, the liquid spray will be saturated and the pressure in the loop will be 0.26 atm. In order to match the subcooling for the 1 atm case, the liquid will need to be thermally subcooled to –12.6 °C (=22-34.6 °C). It is possible for TS to be negative provided noncondensable

Case No.	$T_{reservoir}$ (°C)	T_{spray} (°C)	$P_{reservoir}$ (atm)	T_{sat} (°C)	TS (°C)	GS (°C)	□	Comments
1	23.5	25	0.33	27.1	-1.5	3.6	0.65	Nominally degassed, saturated liquid.
2	22.5	1.4	0.33	27.1	21.1	4.6	0.60	Nominally degassed, thermal subcooling.
3	23.2	25	0.67	45.5	-1.8	22.3	0.73	Gassy subcooling comparable to thermal subcooling of Case 2.
4	24	25	1.0	56.7	-1	32.7	0.73	Test rig at nominally 1 atm, gassy subcooling.
5	24	25	1.22	63.6	-1	39.6	0.83	Test rig above 1 atm, gassy subcooling.

Table 2: Summary of test conditions.

gas is present in the chamber and the liquid is heated to a temperature greater than the reservoir temperature prior to ejection from the spray nozzle. The subcooled state of the liquid being sprayed onto the heater can be characterized by specifying TS and GS.

RESULTS

Results were obtained with the spray nozzle oriented perpendicular to the plane of the microheater array, with the orifice located 17 mm from the surface. All of the heater surface was covered by the spray. The flow rate through the nozzle was set at 37 ml/min. The actual volumetric flux of liquid on the heater was measured by replacing the heater with a plastic insert with a machined hole of the same size and shape as the heater array. The sides of the insert were sloped so that the liquid impacting the insert outside the hole were deflected away from the hole. With the insert spaced 17 mm from the nozzle, the flow rate impacting the heater area was measured to be 11.3 ml/min.

The spray cone angle was measured to from side view photographs of the spray to be about 32°. The size of the drops produced by the nozzle was estimated using a correlation provided by Estes and Mudawar (1995b) for FC-72, FC-87 and water:

$$\frac{d_{32}}{d_0} = 3.67\left[We_{d_0}^{1/2}\,\mathrm{Re}_{d_0}\right]^{-0.259}$$

where $We_{d_0} = \dfrac{\rho_a (2\sigma P)\, d_0}{\sigma}$, $\mathrm{Re}_{d_0} = \dfrac{\rho_f (2\sigma P)^{1/2}\, d_0}{\mu_f}$. The mean absolute error of this correlation was claimed to be 12%. The density ρ_a in We is the density of the ambient fluid into which the liquid is being sprayed. d_{32} was computed from this correlation to vary from 50 μm for Cases 4 and 5 down to 38 μm for Cases 1 and 2.

A summary of the test conditions is presented on Table 2. For Case 5, air was pumped into the flow loop to increase the pressure above atmospheric.

Effect of thermal subcooling on degassed fluid

Spray cooling curves showing the effect of thermal subcooling on nominally degassed fluid are shown on Figure 4, Cases 1 and 2. The heat flux shown is the average heat flux from the middle 64 heaters in the array. Thermal subcooling is seen to increase the heat transfer for a given flow rate due to addition

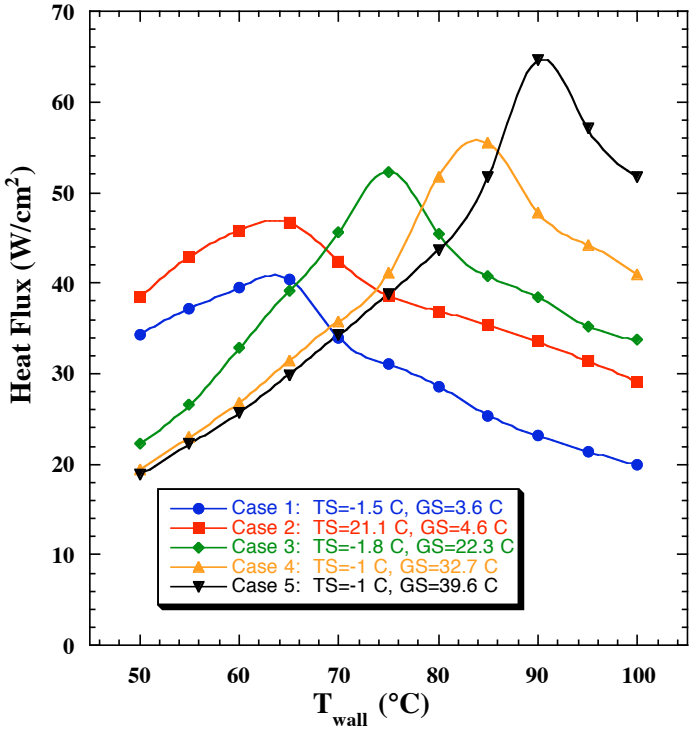

Figure 4: Effect of thermal subcooling and dissolved gas as a function of wall temperature.

of sensible heating required to bring the fluid up to the saturation pressure, and is consistent with the results of previous researchers. The temperature at which CHF occurs increases slightly with thermal subcooling.

Effect of dissolved gas

The effect of varying amounts of dissolved gas on spray cooling at the maximum flow rate tested are also shown on Figure 4. It is observed that as the dissolved gas content increases, the spray cooling curves shift to the right and the CHF increases, consistent with the trends observed by Lin and Ponnappan (2002). The shift to higher temperatures is a direct consequence of the increase in T_{sat} when dissolved gas is present which effectively subcools the liquid. The data for the highest gas content cases (Cases 4 and 5) merge for T_{wall}=50 °C and T_{wall}=55 °C as expected since the wall temperature is below the saturation temperature. Heat is primarily transferred by single-phase convective cooling in this regime, although there may be a some contribution from degassing assisted evaporation, especially considering the high solubility of air in FC-72. The liquid for Case 3 strikes a wall that is slightly

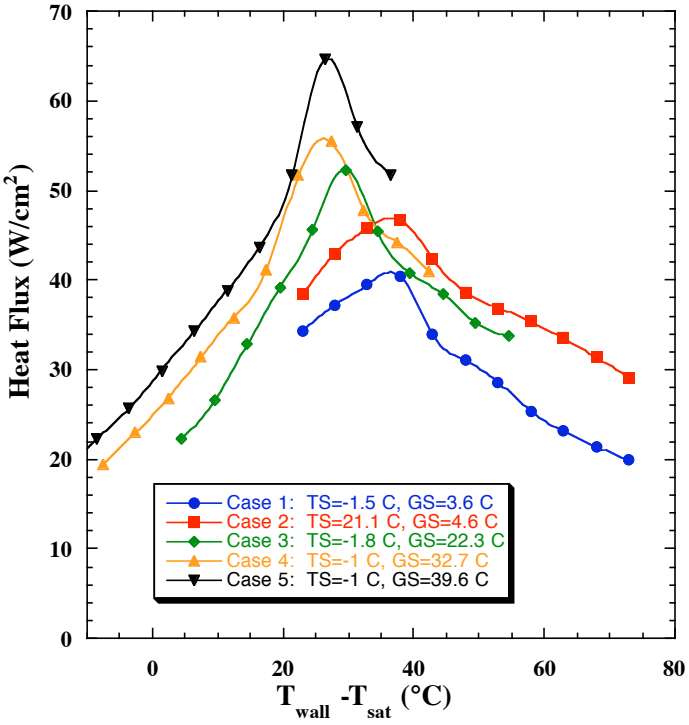

Figure 5: Effect of dissolved gas as a function of wall superheat.

superheated (T_{wall}=50 °C), and this is reflected in the small increase in heat transfer above the data for Cases 4 and 5. The data for Cases 1 and 2 (degassed liquid) are significantly higher, indicating that evaporation plays a major role in spray cooling.

The same heat transfer data plotted vs. wall superheat instead of wall temperature to remove the effect of changes in T_{sat} with gas content is shown on Figure 5. Comparison of Case 2 (S_{tot}=25.7 °C, predominantly thermally subcooled) and Case 3 (S_{tot}=20.5 °C, predominantly gas subcooled) on this figure reveals the role of gas at roughly similar S_{tot} levels. Even though S_{tot} for Case 2 is larger than S_{tot} for Case 3, higher heat transfer is observed for Case 3 at a given superheat, indicating the gas has an effect in addition to the subcooling effect. The presence of gas may cause additional single phase convection over the heater areas not covered by drops, or can contribute additional evaporation of the liquid. The gas may cause bubbles to nucleate within the drops, spreading the drops over a larger heater area thereby increasing the liquid-solid contact area or by increasing the liquid-vapor contact area (as observed in the droplet evaporation experiments of Lee, et al.–2002), increasing the heat transfer. Similar behavior was observed by Cui et al. (2003) in their study of dissolved salt effects on spray cooling heat transfer. They attributed the increase in heat transfer with dissolved salts to increased foaming in the thin liquid film. The gas could also increase the conduction through the drop by reducing the concentration of vapor above the liquid. Modeling of the spray to look at the effects of each of the above is currently in progress, and the results will be presented in the future.

The spray cooling efficiency (η) can be defined as the ratio between the heat transferred from the surface and the heat required to evaporate the liquid completely:

$$\eta = \frac{\dot{q}_w}{\dot{m}\left(c_p \Delta T_{sub} + h_{fg}\right)}$$

The heat transfer from the array was calculated by computing the average heat flux from the inner 64 heaters, then multiplying by the entire heater area to eliminate the effects of substrate conduction from the outer ring of heaters. A summary of η at CHF is summarized on Table 2. Comparison of Cases 1 and 2 indicates that increasing thermal subcooling decreases the efficiency as might be expected since more heat is transferred by the less efficient single phase flow. The presence of gas results in a significant increase in the spray efficiency (compare Cases 2 and 3). In fact, increasing the gas content seems to increase the spray efficiency even though the subcooling increases. The present data suggests that it may be advantageous to operate with dissolved gas if enough condenser area is available or if the volumetric flow of liquid is limited.

Studies of dissolved gas effects on pool boiling heat transfer (e.g., You et al.–1990 and Rainey et al.–2003) have indicated that dissolved gas augments the heat transfer at low wall superheats, but has little effect at higher wall superheats and at CHF. This behavior was attributed to depletion of dissolved gas near the heater surface at higher superheats, resulting in similar heat transfer levels for a given subcooling irrespective of whether the liquid was thermally subcooled or gas subcooled. This is not the case in spray cooling where the thin liquid layer near the heated surface is continually renewed by gassy liquid.

Space resolved heat transfer

An estimate of the heat transfer distribution on the array was obtained by averaging the heat flux over "rings" of heaters for Case 4 (Figure 6). The heat flux from only the operating heaters were considered. The highest heat transfer occurs under the stagnation region at the center of the array, then decreases towards the edges. It is observed that significant non-uniformities in heat transfer exist. Whether this is due to a nonuniform spray droplet distribution or due to interaction between droplets of uniform number density and the near-wall flow field is not currently known. The largest variation in heat transfer occurs at CHF where the heat flux at the center of the array (Ring 1) is 36% higher than on Ring 4. CHF occurs at the highest wall temperature for Ring 1, but the difference in temperature where CHF occurs does not significantly vary across the heater.

Visualization of flow structure

For wall temperatures near T_{sat} or lower, the spray forms a liquid film that covers the majority of the surface. As the wall temperature increases, the film is expected to become thinner due to evaporation. At sufficiently high surface temperatures, the thin film may be disrupted allowing surface tension to pull the liquid into distinct pools. The characteristics of this pooling can be affected by the presence of non-condensable gas as will be discussed below.

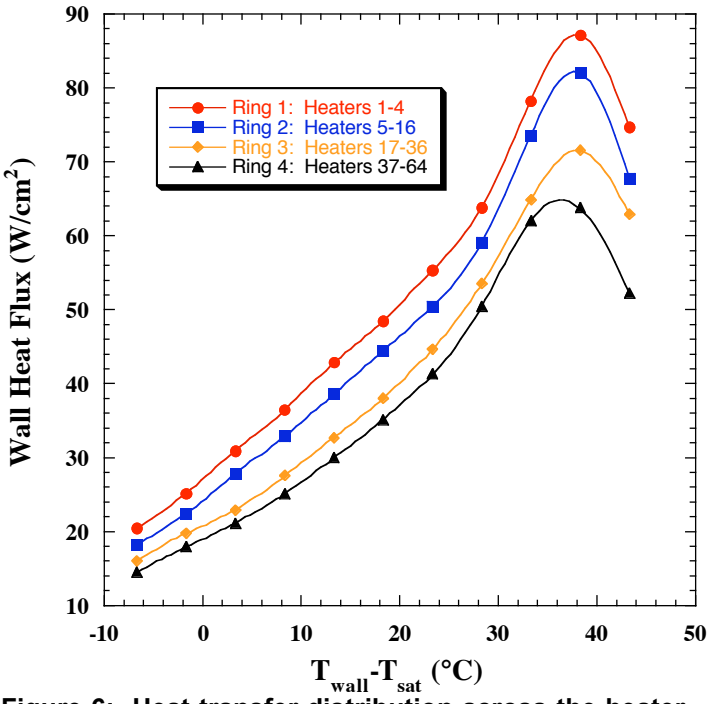

Figure 6: Heat transfer distribution across the heater array for Case 4.

Images of the liquid taken through the heater array at a surface temperature below CHF, near CHF, and above CHF for Case 1 (degassed, low thermal subcooling) are shown on Figure 7. At the lower wall temperature, the liquid on the surface appears to be a mixture of individual droplets and larger distorted pools of moving liquid. Near CHF, many small droplets evenly dispersed over the heater surface are observed. These droplets were observed to slide over the surface. Above CHF, dry patches form where no liquid wets the wall. The location of the dry patches may be influenced by nonuniformities in the temperature across a single heater (the feedback circuits keep only the *average* heat temperature constant), but they appear to be distributed quite uniformly over the heater surface. Dryout does not preferentially occur on the outer edge of the heater array. Images for Case 5 (maximum gas content) are shown on Figure 8. Very few individual droplets are apparent on the images, and most of the liquid is in the form of distorted films. Small dry patches appear to form at CHF, and the dry patches become larger above CHF.

Comparison of Case 2 with Case 3 reveals the effect of gas for similar total subcooling levels. For the low gas case, (Case 2, Figure 9), there are many more identifiable droplets on the surface, with liquid remaining primarily on the heater leads. "Splats" within the liquid pool are occasionally observed, indicating the impact of individual droplets onto the film (middle left edge for the 55 °C and 65 °C cases). The individual droplets are significantly larger than those observed in Case 1 due to the sensible heating required to bring the droplet from its initial temperature to T_{sat}. With gas present (Figure 10), fewer distinct droplets are again observed.

CHF appears to be caused by a fracturing of the film and rapid evaporation of individual droplets when little gas is present. When significant amounts of gas are present, local dry patches within the liquid film appear and grow as the wall temperature increases. The difference between these two cases may be due to the effect of gas on the wettability of the liquid with respect to the surface—increased gas content increases the liquid area in contact with the heater.

CONCLUSIONS

The primary effects of dissolved gas on sprays are to shift the heat transfer curves to higher temperatures by increasing the saturation temperature of the liquid and to increase the CHF level. Although heat transfer is degraded at lower wall temperatures when gas is present, both CHF and spray efficiency increase. Significant non-uniformities in heat transfer across the heater were observed. Visualization of the spray indicate that many single droplets form near CHF when little gas is present. A mixture of individual droplets and larger distorted pools of moving liquid formed with significant levels of gas.

ACKNOWLEDGMENTS

This work was jointly supported by the Laboratory for Physical Sciences (LPS), College Park, MD under Grant No. MDA90499C2618 and the Air Force Research Laboratory (AFRL), Wright Patterson Air Force Base, Dayton, OH under the grant F33615-98-1-2791. The authors wish to express their gratitude to Dr. P. Boudreaux (LPS) and Dr. R. Ponnappan (AFRL) for their encouragement and support throughout this study.

REFERENCES

Chen, R.C., Chow, L.C., Navedo, J.E. (2002), "Effects of Spray Characteristics on Critical Heat Flux in Subcooled Water Spray Cooling", International Journal of Heat and Mass Transfer, Vol. 45, pp. 4033-4043.

Cui, S. Chandra, S. McCahan S. (2000), "Enhanced boiling of water droplets containing dissolved gases or solids", Paper No. NHTC 2000-12249, National Heat Transfer Conference, Pittsburgh, Pennsylvania.

Cui, S., Chandra, S., and McCahan, S., (2003), "The Effects of Dissolving Salts in Water Sprays Used for Quenching a Hot Surface: Part 2–Spray Cooling", Journal of Heat Transfer, Vol, 125, pp. 333-338.

Estes, K.A. and Mudawar, I. (1995a), "Comparison of Two-phase Electronic Cooling Using Free Jets and Sprays", Journal of Electronic Packaging, Vol. 117, pp. 323-332.

Estes, K.A. and Mudawar, I. (1995b), "Correlation of Sauter Mean Diameter and Critical Heat Flux for spray cooling of small surfaces", International Journal of Heat and Mass Transfer, Vol. 38, No. 16, pp. 2985-2996.

Holman, J.P. and Kendall, C.M. (1996), "Spray Cooling Heat-Transfer with Subcooled Trichlorotrifluoroethane (Freon-113) for Vertical Constant Heat Flux Surfaces", HTD-Vol. 333, Proceedings of the ASME Heat Transfer Division, Volume 2.

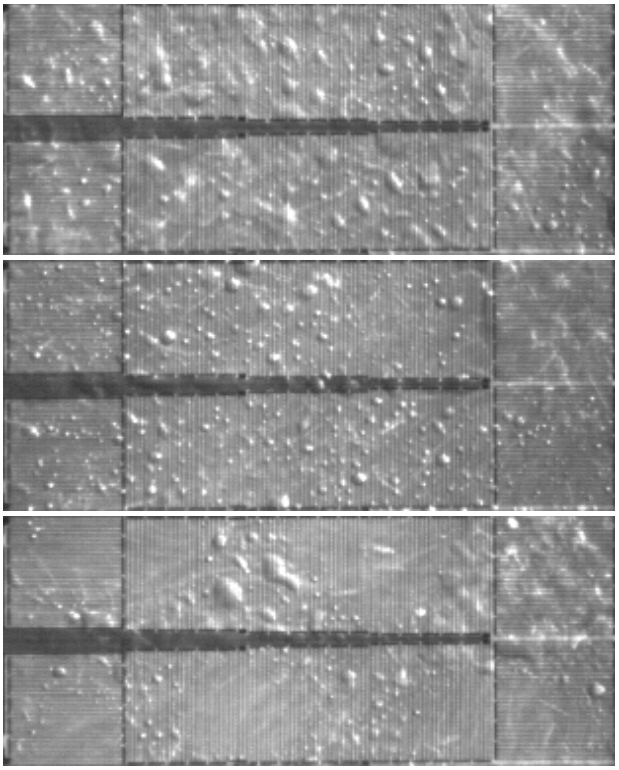

Figure 7: Visualization of Case 1 (degassed, saturated) for wall temperatures around critical heat flux, 55 °C, 65 °C (CHF), and 75 °C (top to bottom respectively).

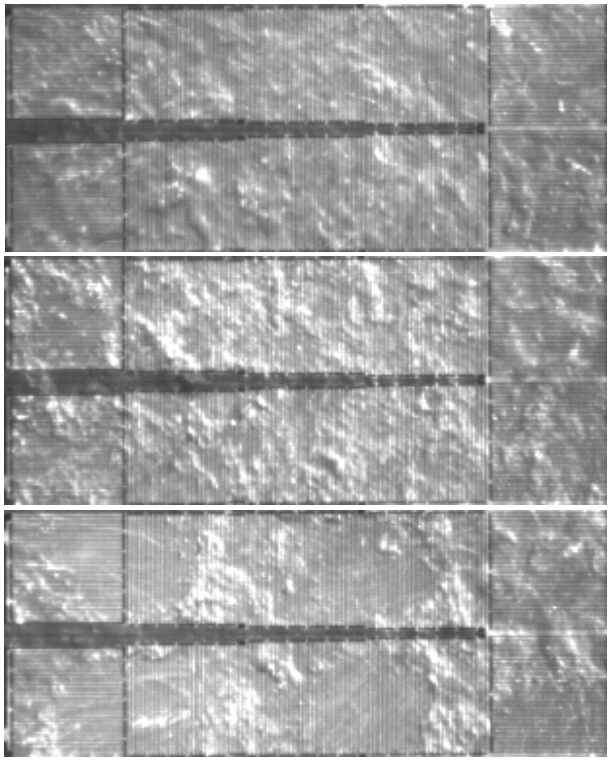

Figure 8: Visualization of Case 5 (high gas concentration) for wall temperatures around critical heat flux, 80 °C, 90 °C (CHF), and 100 °C (top to bottom respectively).

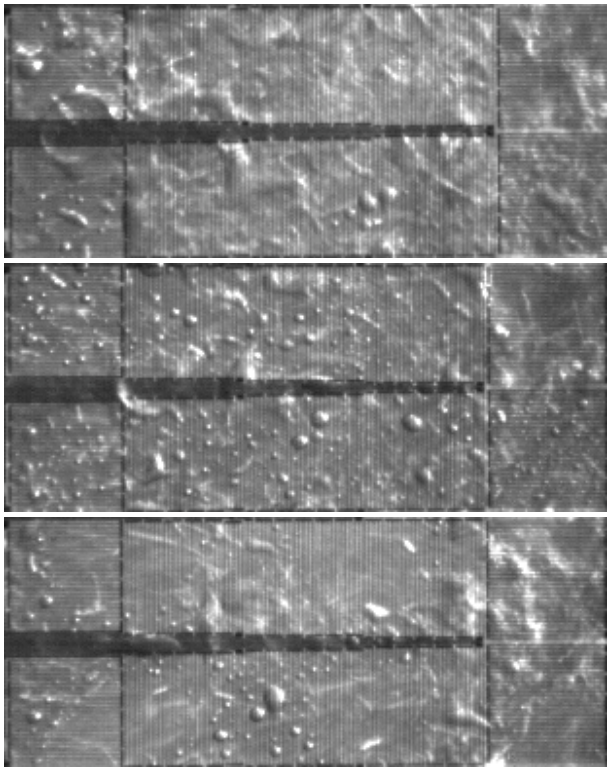

Figure 9: Visualization of Case 2 (degassed, thermal subcooling) for wall temperatures around critical heat flux, 55 °C, 65 °C (CHF), and 75 °C (top to bottom respectively).

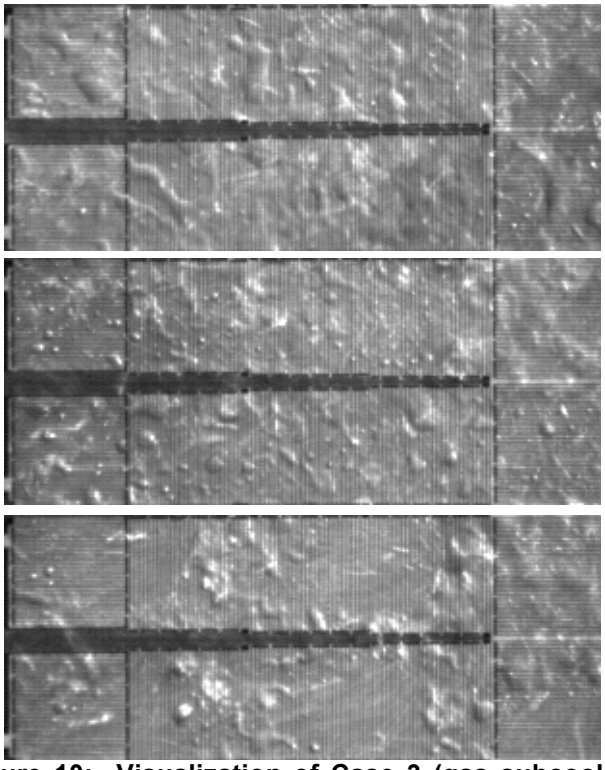

Figure 10: Visualization of Case 3 (gas subcooling similar to thermal subcooling of Case 2) for wall temperatures around critical heat flux, 65 °C, 75 °C (CHF), and 85 °C (top to bottom respectively).

Lee, J., Kiger, K.T, and Kim, J., "Enhancement of Droplet Heat Transfer Using Dissolved Gases", Proceedings of the 2002 SAE Power Systems Conference, Coral Springs, FL, SAE Paper No. 2002-01-3195.

Lin, L, and Ponnappan, R. (2002), "Heat transfer characteristics of an evaporative spray cooling in a closed loop", Proceedings of the 2002 SAE Power Systems Conference, Coral Springs, FL, SAE Paper No. 2002-01-3198.

Milke, J.A., Tinker, S.C., and diMarzo, M., "Effect of dissolved gases on spray evaporative cooling with water", Fire Technology, 2nd Quarter, Vol. 33, No. 2, May/June, 1997.

Ortiz, L and Gonzalez, J.E. (1999), "Experiments on Steady-State High Heat Fluxes Using Spray Cooling", Experimental Heat Transfer, Vol. 12, pp. 215-233.

Rainey, K.N., You, S.M, and Lee, S. (2003), "Effect of Pressure, Subcooling, and Dissolved Gas on Pool Boiling Heat Transfer From Microporous Surfaces in FC-72", Journal of Heat Transfer, Vol 125, pp. 75-83.

Tilton, D.E., Tilton, C.L, Pais, M.R., and Morgan, M.J. (1992) "High-Flux Spray Cooling in a Simulated Multichip Module", HTD-Vol. 206-2, Proceedings of the 1992 ASME Heat Transfer Conference.

You, S.M., Simon, T.W., and Bar-Cohen, A. (1990), "Experiments on Boiling Incipience with a Highly Wetting Dielectric Fluid: Effects of Pressure, Subcooling, and Dissolved Gas Content", Heat Transfer, Proceedings of the International Heat Transfer Conference, Hemisphere, New York, pp. 337-342.